INTRODUCTION TO DIFFRACTION AND LOW X DYNAMICS

E. ELSEN
DESY, Notkestr. 85, D-22603 Hamburg, Germany
E-mail: Eckhard.Elsen@desy.de

An attempt is made to illustrate the relation between low x processes and diffraction. ep scattering provides a unique laboratory, a single hadronic target probed by a point like lepton, where one can try to understand diffraction in terms of a colourless exchange in QCD. Low x processes eventually involve aspects of QCD which cannot be described perturbatively. The HERA inclusive measurements are examined in this respect and compared to results of the Tevatron.

1 Introduction

The geometrical picture of diffraction is one in which the target is (essentially) left intact. The forward scattering amplitude is exponentially suppressed with momentum transfer squared t. The slope b of the distribution, e^{bt} is directly related to the size of the scattering target.

In ep (and pp) scattering diffraction inevitably is also related to low x such that the inelasticity y remains ≈ 1. Low x naturally implies high mass W since in ep scattering $W^2 = Q^2(1-x)/x$. Parton densities at low x have been seen to be large [1]. For large Q^2 there is hence a region of phase space which is calculable perturbatively in QCD even at low x. Figure 1 shows the regions of phase space in a pictorial manner. For very small x initial states of high partonic density are formed. While in these regions methods of perturbative expansion [2,3] have to be proven to be valid it is interesting in its own right to search for experimental evidence for such new partonic configurations. In particular the relation between low x processes and diffraction comes into play.

In diffraction the perturbative exchange has to be colourless and involves at least two gluons. Theoretically the interaction is thus modelled phenomenologically. A particularly useful description is placed in the proton rest frame. At low x the γ emitted from the incoming electron may turn into a $q\bar{q}$-dipole long before the interaction with the proton. The associated formation time $c\tau \sim 1/xm_p$ is typically much larger than the size of the proton target.

Various configurations of the $q\bar{q}$ states may be examined. In *vector meson* production the pair forms a bound state that leaves the interaction unchanged. In *deeply virtual compton scattering* (DVCS) [5] the $q\bar{q}$ state even recombines

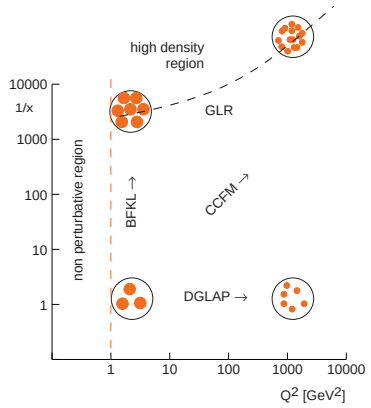

Figure 1. The kinematic plane in ep scattering and an illustration of the parton densities implied and the theoretical approximations deemed to be applicable.

to form a real photon. The study of *inclusive diffraction* enables a test of these dipole configurations under controlled experimental conditions.

Vector meson production has been studied in much detail and a wealth of data both from HERA and the Tevatron have been quantitatively examined in terms of QCD.

2 Geometrical Picture

From its origin in optics diffraction is intimately associated with a geometrical interpretation [4] - the size of the target which participates as a whole. The t-distribution is exponentially suppressed. The energy dependence arises when exciting higher angular momentum states that become accessible with increased phase space. This behaviour is beautifully supported by the observed energy dependence of the total γp-cross section.

Vector mesons exhibit quite distinct variations in their t-behaviour reminiscent of the different sizes at work: from spatially extended ρ mesons to much smaller J/Ψ mesons. It is however interesting to compare the production of vector mesons in elastic and dissociative processes. While the elastic process is only affected by the formation of a vector meson, the dissociative process is modified by the form factor of the proton. Their ratio should hence be independent of the vector meson species. Figure 2 depicts the ratio as a function of the momentum transfer t at the proton vertex, which seems to be

described by a universal behaviour in support of this picture.

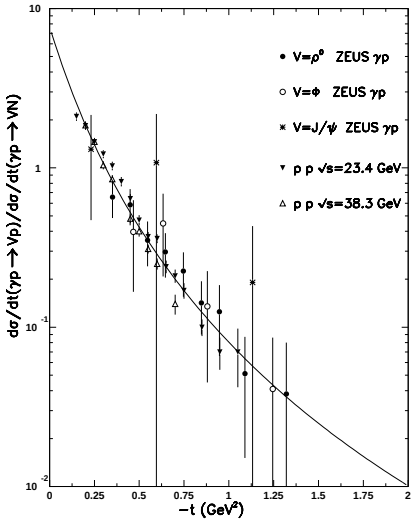

Figure 2. The ratio of elastic to dissociative vector meson production as a function of the momentum transfer t at the proton vertex for γp and pp-data.

3 Inclusive *ep* Scattering

So far the probe has been regarded as a quasi-real photon (without restrictions on transverse dimensions). For $Q^2 \gg 0$ the probe becomes essentially point like and the spatial interplay between probe and target has to be considered. The transition between real photoproduction and deeply inelastic scattering is therefore particularly interesting.

3.1 Inclusive ep Scattering and the low x Behaviour

For Q^2 well below the Z-boson threshold ($Q^2 < M_Z^2$) the cross section

$$\frac{\mathrm{d}\sigma}{\mathrm{d}x\mathrm{d}Q^2} = \left(\frac{2\pi\alpha^2}{Q^4 x}(1+(1-y))^2 F_2 - y^2 F_L\right) \qquad (1)$$

is dominated by the structure function F_2; F_L becoming relevant only at large

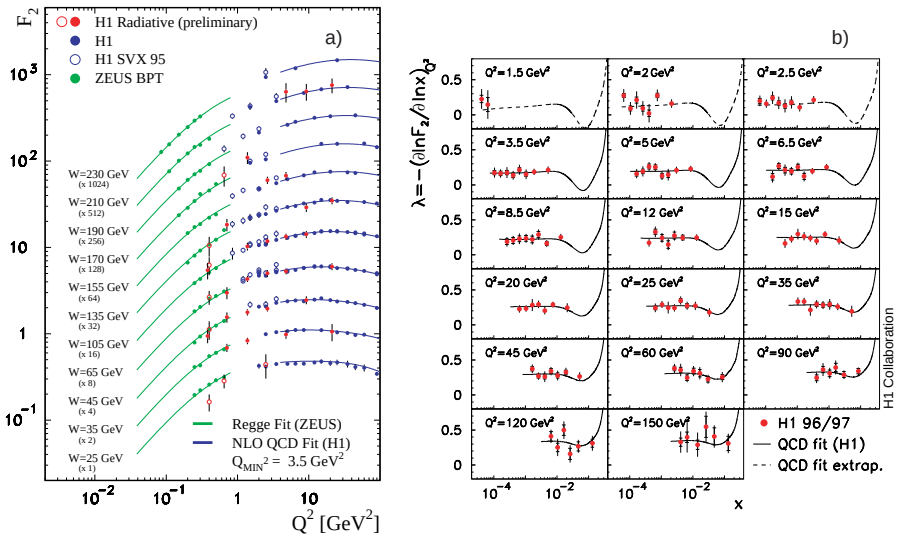

Figure 3. a) The approach to small Q^2 of the structure function F_2. b) The x-derivative of the F_2-structure function vs x. The values λ describe the low x behaviour of the structure function according to $x^{-\lambda}$.

y and at small Q^2. Figure 3a) shows the transition of F_2 towards photoproduction where F_2 has to vanish $\propto Q^2$ to yield a finite $\gamma^* p$ cross section. While the region $Q^2 > 1\,\mathrm{GeV}^2$ is well described by recent QCD fits, the region below $1\,\mathrm{GeV}^2$ relies on Regge inspired fits typically involving vector meson formation. For the region explored the energy dependence is smooth. There are no explicit signs of alteration of the behaviour as a function of $x \sim Q^2/W^2$.

It is therefore interesting to study the small x behaviour of the structure function for not so small Q^2, i.e. the region related to the high energy behaviour of the scattering process and accessible to perturbative methods. Figure 3b) depicts the derivative

$$\lambda = -\left(\frac{\partial \ln F_2}{\partial \ln x}\right)_{Q^2} . \tag{2}$$

The distribution is experimentally consistent with being constant for $x < 0.01$ over a large range in Q^2. The implication $F_2 = c(Q^2)x^{-\lambda}$ then yields a value for λ that rises linearly with Q^2 (cf. figure 4a)) quite different from the

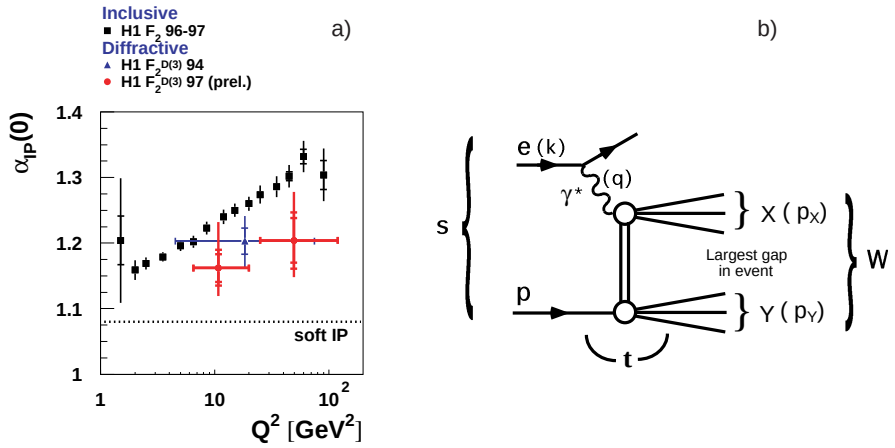

Figure 4. a) the Q^2-dependence of the Pomeron intercept $\alpha_{I\!P}(0) = 1 + \lambda$. Shown in red is the value derived from inclusive diffractive scattering, cf. section 3.2. The diagram b) illustrates the definition of the signature for selection of diffractive events based on the signature of a large gap in rapidity.

photoproduction value $\lambda = 0.08$. In the Regge language of *Pomeron* exchange the exchange becomes harder the larger Q^2.

3.2 Inclusive diffraction

Characteristic of the diffractive interaction is the large region void of hadronic activity - a gap in rapidity between the forward going nucleon and the centrally detected final state X, cf. figure 4b). Such a selection procedure leads to an inclusive measurement. Figure 5 shows the fraction $\rho^{D(3)}(\beta, Q^2, x_{I\!P}) = M_X^2 x/Q^2 \cdot F_2^{D(3)}(\beta, Q^2, x_{I\!P})/F_2(x, Q^2)$ of diffractively produced events as a function of Q^2 and x. With $\beta \approx Q^2/(Q^2 + M_X^2)$ and for two intervals of $x_{I\!P} \approx (Q^2 + M_X^2)/(Q^2 + W^2)$ the fraction of diffractive events is considerable and the production persists up to the largest values of Q^2 of $60\,\mathrm{GeV}^2$ investigated. When analyzing the diffractive exchange in terms of a partonic description in QCD one finds a large gluonic component [6]. To understand the formation of the final state more explicit final state measurements have to be investigated.

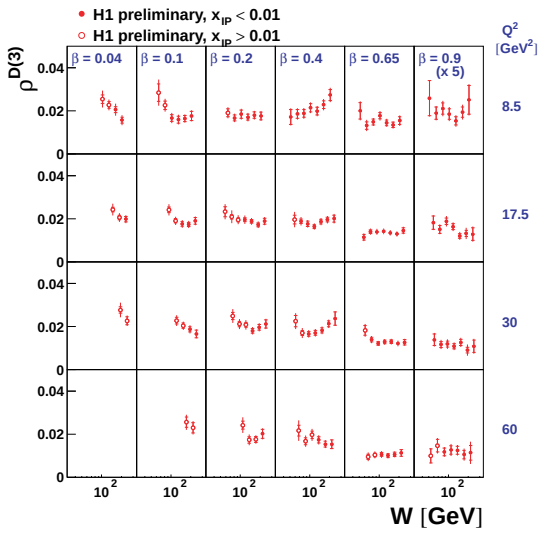

Figure 5. The ratio $\rho^{D(3)}$ of the diffractive to inclusive structure function for two ranges of $x_{I\!P}$ from [6].

3.3 Inclusive Diffraction of Charm Mesons and Jets

Charm mesons originate from gluonic interactions and are hence a sensitive probe of the gluonic content of the interaction. Figure 6 (left) demonstrates a large charm component in diffractive processes. Similarly, multi-jet formation involves several partons. From an analysis of such final states, cf. figure 6 (right) one may conclude on the dynamical characteristics of the diffractive process. - As becomes evident, the description thus achieved is satisfactory and indicative of the large gluon content.

4 Comparison to Tevatron Jets

The observations are quite at variance to the understanding of diffraction at the Tevatron. In pp scattering the density of hadronic matter is so large that an initially formed gap is not likely to survive unaffectedly the remainder of the transition through hadronic matter. The application of the partonic description of diffractive ep data thus leads to a gross overestimate of the production at the Tevatron, cf. figure 7. The environment of hadron-hadron scattering is less amenable to a theoretical understanding of diffraction.

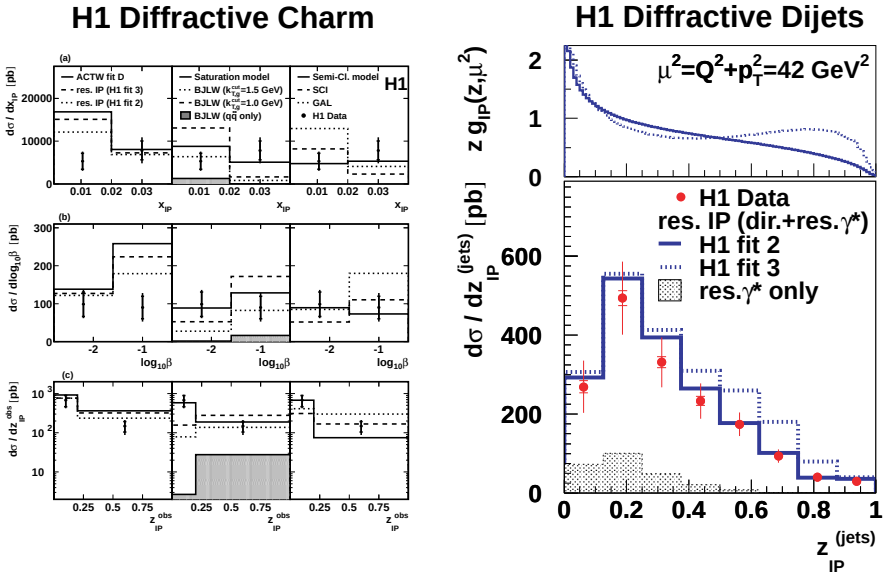

Figure 6. Production of (left) charm and (right) jets in diffraction as a function of the momentum fraction $z_{I\!P}$.

5 Conclusion

As wealth of data has been amassed at HERA and the Tevatron on low x physics and diffractive processes [8–10]. The HERA data provide the clues on further understanding of high density (partonic) final states which to some extent are a prerequisite for diffractive interaction to take place. While at HERA diffractive production can be understood in terms of QCD the Tevatron data show that more complex mechanisms are at work in hadron-hadron scattering. The reach to low x currently available at HERA does not yield experimental evidence for saturation of partonic matter density.

Acknowledgments

I wish to thank organisers of the 31st ISMD for a very pleasant stay in Datong and the kind hospitality extended to the participants. Special thanks go to Liu Lianshou, Wu Yuanfang and Frans Verbeure for organizing the symposium and to Jim Crittenden for arranging a very fruitful session on diffraction.

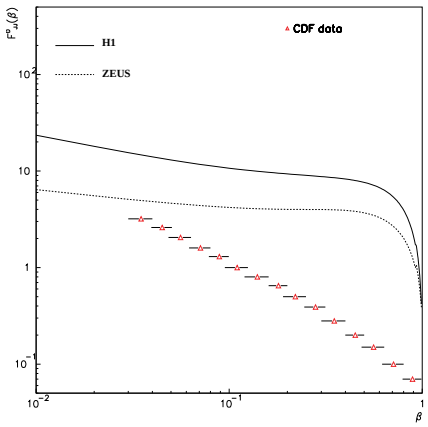

Figure 7. Comparison of diffractive dijet production at the Tevatron with the expectations from parameterizations of the HERA measurements [7].

References

1. I. Abt *et al.* [H1 Collaboration], Nucl. Phys. B **407** (1993) 515;
   M. Derrick *et al.* [ZEUS Collaboration], Phys. Lett. B **316** (1993) 412.
2. Yu.L. Dokshitzer, Sov. Phys. JETP **46** (1977) 641;
   V.N. Gribov, L.N.Lipatov, Sov. J. Nucl. Phys. **15** (1972) 438 and 675;
   G. Altarelli, G. Parisi, Nucl. Phys. **B126** (1977) 298.
3. E.A. Kuraev, L.N. Lipatov, V.S. Fadin, Sov. Phys. JETP **44** (1976) 443;
   E.A. Kuraev, L.N. Lipatov, V.S. Fadin, Sov. Phys. JETP **45** (1977) 199;
   Y.Y. Balitsky, L.N. Lipatov, Sov. Journ. Nucl. Phys. **28** (1978) 822.
4. J. Bartels and H. Kowalski, Eur. Phys. J. C **19** (2001) 693.
5. C. Adloff *et al.* [H1 Collaboration], Phys. Lett. B **517** (2001) 47.
6. P. Newman, "Measurements of the Diffractive Structure Function F_2^D at HERA", Proceedings of *EPS Conference*, Budapest 2001.
7. C. Royon *et al.*, Phys. Rev. D **63** (2001) 074004.
8. A.A. Savin, XXXI ISMD, Datong 2001, these proceedings.
9. D. Milstead, XXXI ISMD, Datong 2001, these proceedings.
10. L. Demortier, XXXI ISMD, Datong 2001, these proceedings.